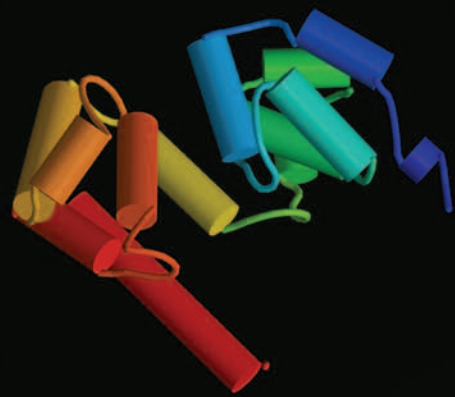
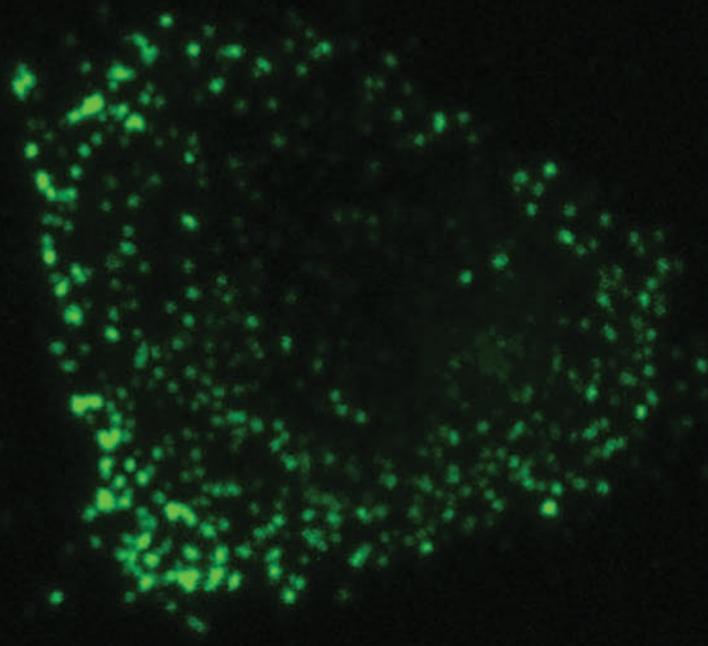
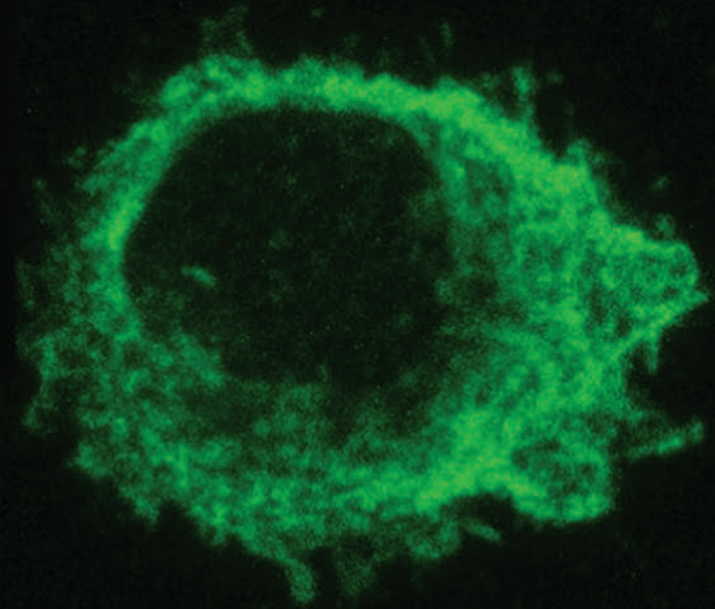


Molecular Cell

Volume 20 Number 6

December 22, 2005



FLIP Structure and Function

Crystal Structure of MC159 Reveals Molecular Mechanism of DISC Assembly and FLIP Inhibition

Jin Kuk Yang,^{1,3} Liwei Wang,^{1,3} Lixin Zheng,²
Fengyi Wan,² Misonara Ahmed,¹
Michael J. Lenardo,² and Hao Wu^{1,*}

¹Department of Biochemistry
Weill Medical College of Cornell University
1300 York Avenue
New York, New York 10021

²Laboratory of Immunology
National Institute of Allergy and Infectious Diseases
National Institutes of Health
Bethesda, Maryland 20892

Summary

The death-inducing signaling complex (DISC) comprising Fas, Fas-associated death domain (FADD), and caspase-8/10 is assembled via homotypic associations between death domains (DDs) of Fas and FADD and between death effector domains (DEDs) of FADD and caspase-8/10. Caspase-8/10 and FLICE/caspase-8 inhibitory proteins (FLIPs) that inhibit caspase activation at the DISC level contain tandem DEDs. Here, we report the crystal structure of a viral FLIP, MC159, at 1.2 Å resolution. It reveals a noncanonical fold of DED1, a dumbbell-shaped structure with rigidly associated DEDs and a different mode of interaction in the DD superfamily. Whereas the conserved hydrophobic patch of DED1 interacts with DED2, the corresponding region of DED2 mediates caspase-8 recruitment and contributes to DISC assembly. In contrast, MC159 cooperatively assembles with Fas and FADD via an extensive surface that encompasses the conserved charge triad. This interaction apparently competes with FADD self-association and disrupts higher-order oligomerization required for caspase activation in the DISC.

Introduction

Death receptors (DRs) in the Tumor Necrosis Factor (TNF) Receptor (TNFR) superfamily mediate the extrinsic pathway of apoptosis and play critical roles in embryonic development, cellular homeostasis, and immune regulation (French and Tschoop, 2003; Locksley et al., 2001; Peter and Kramer, 2003; Wajant, 2002). Current members of the DR subfamily include Fas (also known as CD95 and APO-1), TNF-R1, DR3, TRAIL-R1, TRAIL-R2, DR6, EDA-R, and NGF-R (French and Tschoop, 2003). Signaling by these receptors is triggered by interaction with one or more specific ligands that are members of the TNF superfamily. Genetic mutations or abnormal expression of DRs and their ligands have been associated with many human diseases including the Autoimmune Lymphoproliferative Syndrome (ALPS), cancer, and tissue destructive diseases such as graft-versus-host disease, multiple sclerosis, and stroke

(French and Tschoop, 2003). Highly effective therapeutics for modulating DR signaling have emerged. These include antagonistic antibodies in tissue destructive diseases and agents that selectively trigger DR-mediated cell death in cancer cells (French and Tschoop, 2003). Therefore, a detailed understanding of the signaling and regulatory mechanisms of DRs has broad medical and biological importance.

DR signaling is mediated by highly specific protein-protein associations that generate oligomeric signaling assemblies such as the DISC (Kischkel et al., 1995; Wajant, 2002). DRs contain a DD in their intracellular regions (Itoh and Nagata, 1993; Tartaglia et al., 1993; Wajant, 2002). For Fas, its DD recruits the FADD adaptor protein via a homotypic interaction with the C-terminal DD of FADD (Chinnaiyan et al., 1995; Kischkel et al., 1995). FADD also contains an N-terminal DED that interacts homotypically with the tandem DEDs in the prodomains of caspase-8 or -10 (Boldin et al., 1996; Muzio et al., 1996). These interactions form the ternary DISC that contains Fas, FADD, and caspase-8 or -10. Recruitment of procaspases into the DISC initiates proteolytic autoprocessing (Medema et al., 1997; Salvesen and Dixit, 1999; Shi, 2004). This liberates active caspase-8 or -10 into the cytoplasm to cleave and activate effector caspases such as caspase-3 and caspase-7, leading to a cascade of events in apoptotic cell death (Salvesen, 2002).

In addition to caspase-8 and -10, most FLIPs are also tandem DED-containing proteins, which regulate DISC assembly and caspase activation (Thome and Tschoop, 2001). Cellular FLIPs (cFLIPs), comprising the long and short isoforms cFLIP(L) and cFLIP(S), are tightly regulated in expression in T cells and might be involved in the control of both T cell activation and death (Goltsev et al., 1997; Han et al., 1997; Hu et al., 1997b; Inohara et al., 1997; Irmiler et al., 1997; Rasper et al., 1998; Shu et al., 1997; Srinivasula et al., 1997; Thome and Tschoop, 2001). Viral FLIPs (vFLIPs) appear to have evolved to inhibit apoptosis of infected host cells and are present in the poxvirus *Molluscum contagiosum virus* (MCV) (Bertin et al., 1997; Garvey et al., 2002b; Hu et al., 1997a; Shisler and Moss, 2001; Thome et al., 1997) and γ -herpesviruses such as equine herpesvirus-2 (EHV-2), herpesvirus saimiri (HVS), the Kaposi-associated human herpesvirus-8 (HHV-8), and rhesus rhadinovirus (RRV) (Bertin et al., 1997; Hu et al., 1997a; Searles et al., 1999; Thome et al., 1997; Thome and Tschoop, 2001).

The DDs and DEDs involved in DR signaling are members of the DD superfamily, which also includes the caspase recruitment domains (CARDs) involved in the intrinsic cell death pathway and the Pyrin domains (PYDs) involved in inflammatory signaling (Kohl and Grutter, 2004; Reed et al., 2004). The DD superfamily contains homotypic protein-protein interaction modules. NMR structures of the first DD (Huang et al., 1996), DED (Eberstadt et al., 1998), CARD (Chou et al., 1998), and PYD (Hiller et al., 2003) have all revealed a common six-helical bundle structure. Despite their biological importance, there are currently no reported structures of tandem

*Correspondence: haowu@med.cornell.edu

³These authors contributed equally to this work.

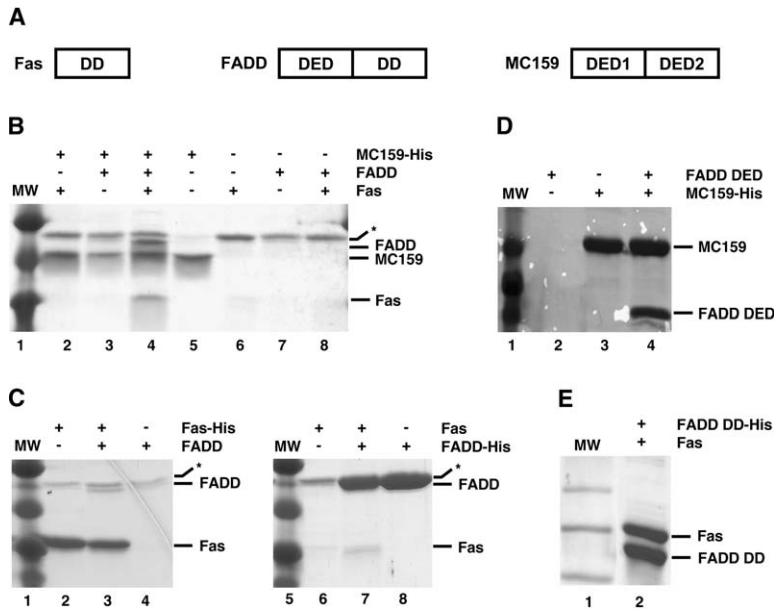


Figure 1. Cooperative Assembly of Fas, FADD, and MC159

(A) Schematic domain organization of Fas, FADD, and MC159 is shown.

(B) His-tag pull-down of MC159, Fas DD, and FADD is shown.

(C) His-tag pull-down of Fas DD and FADD.

(D) His-tag pull-down of MC159 and FADD DED.

(E) His-tag pull-down of Fas DD and FADD DD.

Contaminants are marked by an asterisk.

DEDs. Both the architectural features of the individual DEDs in tandem DEDs and the mode of their association are entirely unknown. Therefore, the molecular basis for the recruitment of caspase-8, caspase-10, and FLIPs remains to be revealed.

To elucidate the molecular basis for the functions of tandem DED-containing proteins, we determined the crystal structure of MC159, a vFLIP from MCV, at 1.2 Å resolution. It reveals a dumbbell-shaped structure with rigidly associated DED1 and DED2 via hydrophobic interactions. DED1 is highly divergent from DED2 and other DED structures. The DED1/DED2 interaction is topologically different from the previously observed CARD/CARD and DD/DD interactions (Qin et al., 1999; Xiao et al., 1999). A hydrogen-bonded charge triad is present on the surface of DED1 and DED2, which may represent a general characteristic feature of DEDs, but not other members of the DD superfamily. We found that the conserved hydrophobic patch of DED2 mediates caspase-8 recruitment and DISC assembly. Similar mechanisms might be used by cFLIPs and herpesvirus vFLIPs to compete with caspase-8 recruitment. In contrast to hydrophobic interactions, MC159 uses an extensive charge surface that encompasses the charge triad to cooperatively assemble with Fas and FADD. This interaction does not compete with caspase-8 recruitment, but apparently competes with FADD self-association and disrupts higher order oligomerization required for caspase activation in the DISC. Together, these structural, biochemical, and mutational studies reveal important insights into the molecular mechanism of DISC assembly and FLIP inhibition.

Results

Fas, FADD, and MC159 Are Cooperatively Assembled into a Ternary Complex

We used recombinant proteins and a His-tag pull-down assay to establish an *in vitro* system for assessing the recruitment of MC159. MC159 interacted effectively

with Fas DD and FADD, as shown by the pull-down of an apparent ternary complex with His-tagged MC159 (Figure 1B, lane 4). However, in the absence of Fas DD, His-tagged MC159 only weakly pulled down FADD (Figure 1B, lane 3) and, in the absence of MC159, Fas DD only weakly interacted with FADD (Figure 1C, lanes 3 and 7). These data suggest that the binary Fas DD/FADD and FADD/MC159 interactions are weak and that the ternary complex is cooperatively assembled.

Because isolated FADD DED interacted strongly with MC159 (Figure 1D, lane 4) and isolated FADD DD interacted strongly with Fas DD (Figure 1E, lane 2), it appears that the DED in full-length FADD autoinhibits its DD from interacting effectively with Fas DD and that the DD in full-length FADD autoinhibits its DED from interacting strongly with MC159. This autoinhibition is relieved when the third component of the complex is present.

High-Resolution Structure of MC159: Noncanonical Fold of DED1 and the Charge Triad

To elucidate the molecular basis of DISC assembly and FLIP-mediated inhibition of caspase activation, we determined the crystal structure of MC159, a vFLIP from MCV (Figure 2, Table 1). The structure of full-length MC159 was first solved at 3.8 Å resolution by single-wavelength anomalous diffraction and 4-fold noncrystallographic symmetry averaging (Figure 2A). It revealed that more than fifty residues at the C-terminal tail of MC159 were disordered in the crystal. By removing this region of MC159, a different crystal form that diffracted to 1.2 Å resolution was obtained (Figure 2B). The original atomic model built from the low-resolution crystal form was used to determine the structure of the high-resolution crystal form. Structural analyses are based on information from the high-resolution structure.

The tandem DEDs of MC159 form a dumbbell-shaped structure with each DED as the weight at either end (Figure 2C). Although all members of the DD superfamily appear to exhibit the fold of a six-helical bundle, DED1 is highly divergent from DED2 and the known NMR

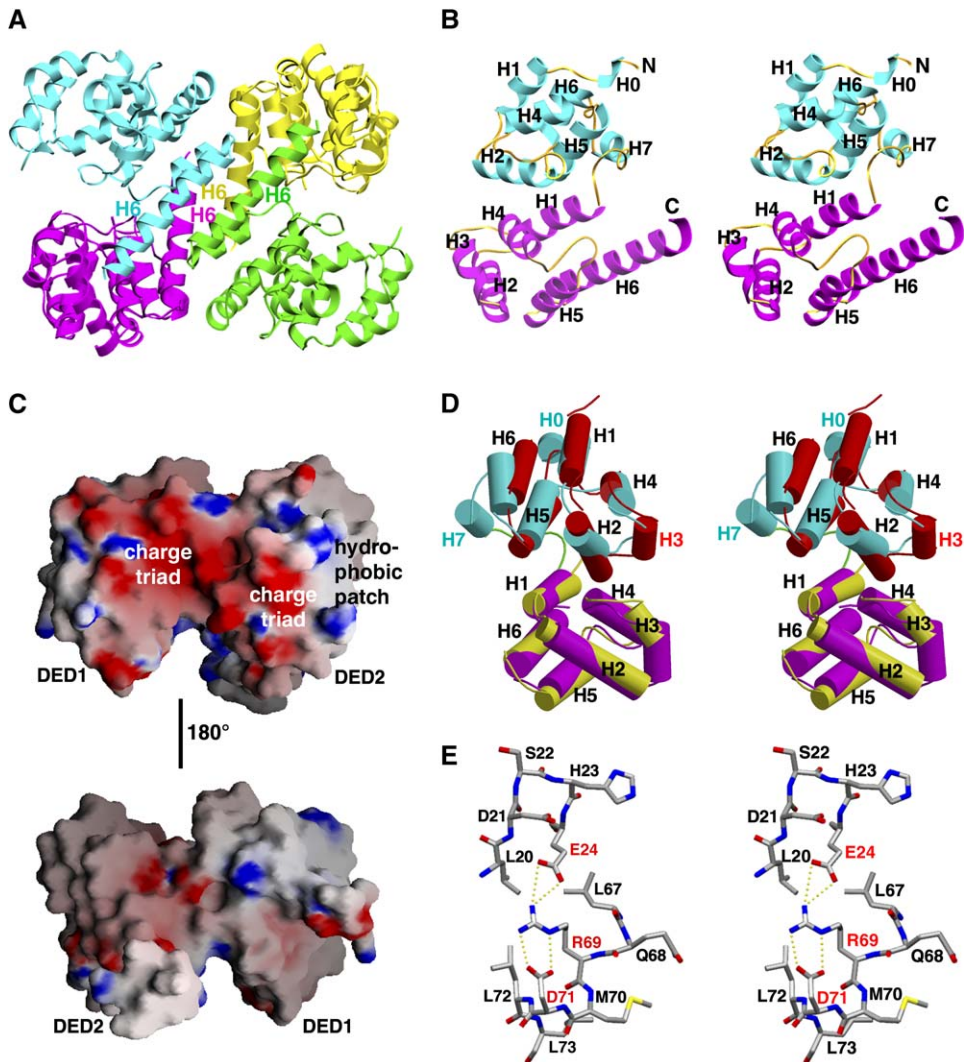


Figure 2. Crystal Structure of MC159

(A) MC159 tetramer structure from the P222₁ crystal form is shown in cyan, magenta, yellow, and green, respectively, for each monomer. (B) Stereo ribbon drawing of the high-resolution structure of MC159 from the P2₁2₁2₁ crystal form. DED1 is shown in cyan and DED2 in magenta. Helices H0-H7 of DED1 and H1-H6 of DED2 are labeled. H3 is absent in DED1. (C) Electrostatic surface representation of MC159, showing the dumbbell-shaped structure and the rich charges on one face of MC159. The top panel is related to (B) by an ~180° rotation along the vertical axis followed by a 90° rotation on the page. The lower panel is related to (B) by an ~90° rotation on the page. (D) Stereo cylinder drawing showing the superposition of MC159 DED1 (cyan) with FADD DED (red) and DED2 (magenta) with FADD DED (yellow). For the superposition between DED1 and FADD, helices H0 and H7 are only present in DED1, whereas H3 is only present in FADD. (E) Stick model for the hydrogen bonding interactions in the charge triad of DED1 is shown.

structures of single DEDs from FADD (Eberstadt et al., 1998) and PEA-15 (Hill et al., 2002) (Figure 2D, see Table S1 in the Supplemental Data available with this article online). In particular, the topologically equivalent helix H3 is missing, which is replaced by a short loop connecting helices H2 and H4. This loop is mostly hydrophilic and does not contribute to the hydrophobic core of DED1. Two additional helices are present, helix H0 at the N terminus and helix H7. Helix H7 covers helix H5 and helps to close the hydrophobic core of the domain. It also brings the chain to the beginning of DED2. In addition, DED1 has a shorter helix H2 and a different orientation in helix H6. Only about half of the residues in DED1 were aligned within 3 Å in C α distance to DED2, FADD DED, and PEA-15 DED (Table S1). In fact, a DALI struc-

tural homology search (Holm and Sander, 1995) showed that DED1 structure is almost as different to these DED structures as to other structures in the DD superfamily such as those of DDs, PYDs, and CARDS (Table S1).

On the other hand, DED2 is a bona fide DED. It showed extensive structural homology with the known DED structures from FADD and PEA-15, which were also the top two matches from a structural homology search with DALI (Figure 2D, Table S1). Among the 97 residues in DED2, 74 residues were aligned with FADD and PEA-15 to within 3.0 Å in C α distance, giving rise to RMSDs of 1.4 Å in both cases (Table S1). All six canonical helices are present in DED2. In comparison with FADD DED, the helices H1, H4, H5, and H6 of DED2 are more conserved structurally, whereas helices H2 and H3 show more

Table 1. Crystallographic Statistics

	SeMet (Residues 1–241)	Native (Residues 1–187)
Data Collection		
Space group	P222 ₁	P2 ₁ 2 ₁ 2 ₁
Cell dimensions a, b, c	84.0 Å, 108.2 Å, 142.7 Å	35.0 Å, 62.9 Å, 75.8 Å
Resolution	30–3.8 Å	15–1.2 Å
R _{sym}	8.4% (35.3%)	5.9% (30.7%)
I/σI	20.0 (3.5)	48.5 (4.4)
Completeness	99.7 (98.6%)	99.6% (97.9%)
Redundancy	6.5 (4.5)	6.7 (4.2)
Refinement		
Resolution		15–1.2 Å
Number of reflections		51,463
R _{work} /R _{free}		21.2%/23.3%
Number atoms		
Protein/water and other small molecule		1492/322
Average B factors		
Protein/water and other small molecule		15.8 Å ² /33.5 Å ²
Rms deviations		
Bond lengths/angles		0.0037 Å/0.99°
Ramachandran plot		
Most favored/ additionally allowed		93.9%/6.1%

Highest resolution shell is shown in parenthesis.

variations in position. Helix H6 is exceptionally long in DED2; it comprises 21 residues and runs to the end of the construct at residue 187. Approximately half of helix H6 does not pack against the core of DED2; instead it protrudes prominently. In the low-resolution crystal form, helix H6 is involved in the organization of four MC159 molecules in an almost perfect 222 noncrystallographic symmetry (Figure 2A). However, MC159 is a monomer in solution and the tetrameric association does not appear to have any biological significance. Previous truncation studies have shown that a large part of helix H6 could be truncated (up to residue 179) without affecting its apoptosis protection function (Garvey et al., 2002a), and mutations of exposed residues on the remaining part of H6 did not affect ternary complex formation with Fas and FADD (see below).

The high-resolution structure of MC159 revealed a hydrogen-bonded charge triad on the surface of DED1 and DED2 (Figure 2E, Table S2), which contributes to the highly charged features on one face of the structure (Figure 2C). We refer the charge triad as the E/D-RxDL motif (“x” for any amino acid). It involves the Arg and Asp residues in the RxDL motif in helix H6 (residues 69–72 in DED1 and residues 166–169 in DED2) and a negatively charged residue in helix H2 (E24 in DED1 and E111 in DED2). The RxDL motif was previously shown to be functionally important (Garvey et al., 2002b). Extensive hydrogen bonding interactions are observed among these charged side chains. In DED1, for example, Arg69 situates in between Asp71 and Glu24. All three polar atoms in the Arg69 side chain make hydrogen bonds: N ϵ and N η 2 with the O δ 1 and O δ 2 atoms of Asp71 and N η 1 with O ϵ 1 and O ϵ 2 of Glu24 with perfect hydrogen bonding distances. These hydrogen bonds likely help to maintain a precise organization of the

side chains, which may be functionally important (see below). It is also possible that they play a local structural role in maintaining the conformation of this region of the DEDs. The charge triad is highly conserved in most single and tandem DEDs (Figure 3A), but is not present in other members of the DD superfamily, suggesting that it is a characteristic feature of DEDs alone. Interestingly, the charge triad is conspicuously altered or missing in three of the four DEDs in caspase-8 and caspase-10. In caspase-8 DED2, the E/D-RxDL motif has a Glu, Lys, and Ser at the three charged residue positions, and “x” is missing. It is possible that the change from Arg to Lys lowers the hydrogen bonding potential so it now only interacts with one negatively charged residue in the triad. For caspase-10, the E/D-RxDL motif is missing in both DED1 and DED2. It is possible that this motif does not play an important role in caspase recruitment but is important in other functions of DED-containing proteins (see below).

The Interaction between DED1 and DED2 Reveals a Conserved Rigid Tandem DED Association and a Different Mode of Interaction in the DD Superfamily

Unlike beads on a string, the structure of MC159 revealed that DED1 and DED2 are rigidly associated with each other in a compact structure (Figures 2B and 2C). The DED1/DED2 interface is extensive, burying approximately 1380 Å² of surface area. The two DEDs are related, very approximately, by a translation across the contact interface so that one side of DED1 is contacting the equivalently opposite side of DED2. The translational relationship between DED1 and DED2 is made possible by helix H7 of DED1.

The interaction at the DED1/DED2 interface is mostly hydrophobic, mediated by helices H2 and H5 of DED1 and helices H1 and H4 of DED2 (Figures 3B and 3C). There are a total of 195 interfacial atomic contacts, among which 117 are between nonpolar atoms, 17 are between polar atoms, and 61 are mixed contacts between polar and nonpolar atoms. The surface patch formed by H2 and H5 of DED1 is equivalent to the conserved hydrophobic patch identified on the surface of FADD DED that is important for caspase-8 interaction (Eberstadt et al., 1998) (Figure 3A). The H1 and H4 surface of DED2 is equivalent to the second hydrophobic patch identified in the FADD DED structure on the opposite side, which does not appear to be important in FADD signaling (Eberstadt et al., 1998). In addition to hydrophobic interactions, three interfacial hydrogen-bonding networks are observed (Figure 3C). The first one is the salt bridge between Asp34, localized between H2 and H4 of DED1, and Arg97 in H1 of DED2. The second one involves the side chains of H23 and S26 in H2 of DED1, Glu105 in H1 of DED2, and Arg135 in the H3-H4 loop of DED2. The last one is the salt bridge between Glu62 in H5 of DED1 and Lys98 in H1 of DED2. The interfacial residues, especially those that are completely buried at the DED1/DED2 interface and contribute large surface areas, such as F30, L31, F92, L93, and R97, are mostly conserved in tandem DEDs (Figure 3A). This suggests that all known tandem DEDs form a similar rigid compact structure as MC159.

The observed interaction between DED1 and DED2 represents an example of a DED/DED interaction.

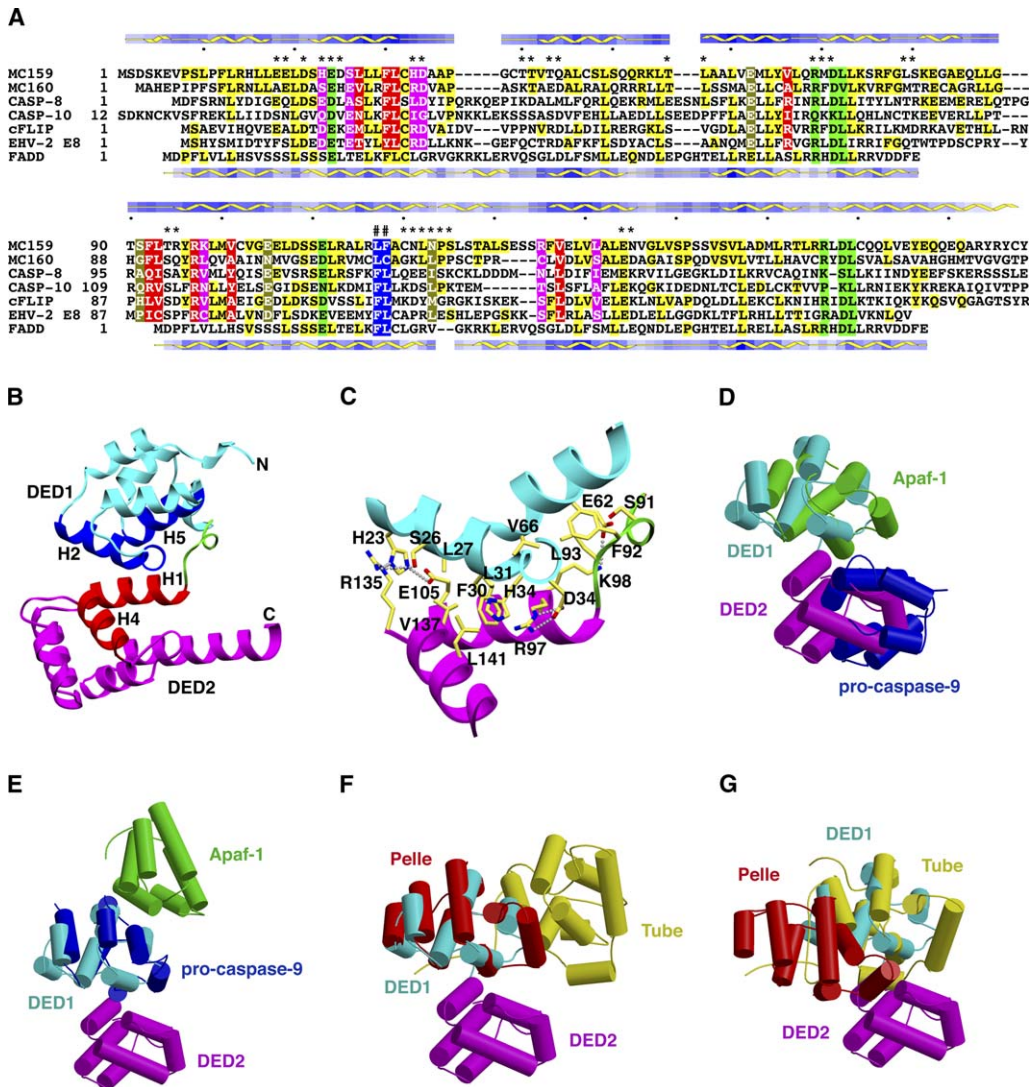


Figure 3. Mode of Interaction between DED1 and DED2

(A) Sequence alignment of MC159 with other tandem DED-containing proteins and structure-based sequence alignment with FADD. Residues with more than 40 Å² surface area buried at the DED1/DED2 interface are shaded in red (completely buried) and magenta (partially buried) and residues with 30–40 Å² surface area buried at the DED1/DED2 interface are shaded in brown. Residues at the charge triad E/D/-RxDL motif positions are shaded in green, and residues at the conserved hydrophobic patch of DED2 are shaded in blue. Residues of MC159 involved in FADD interaction are marked by an asterisk. Residues of caspase-8 involved in FADD interaction are marked by “#”. Sequences identical to MC159 are shaded in yellow. Secondary structures of MC159 and FADD are shown above and below the sequences, respectively. Different shades of blue bars indicate whether a residue is buried (dark blue) or exposed (light blue). Abbreviations are as follows: CASP-8, caspase-8; CASP-10, caspase-10; cFLIP, cFLIP(S); EHV-2 E8, vFLIP from equine herpesvirus-2.

(B) Regions of MC159 involved in the interaction are shown in blue for DED1 (residues 22–35 and 57–66), red for DED2 (residues 94–105 and 135–145), and green for the DED1-DED2 linker (residues 86–94).

(C) Detailed interaction between DED1 and DED2. Potential hydrogen bonds are shown by dotted lines.

(D and E) Comparison of DED1/DED2 interaction with the Apaf-1 CARD/pro-caspase-9 CARD interaction is shown. Apaf-1 and pro-caspase-9 in the Apaf-1/pro-caspase-9 complex are each superimposed with DED1, respectively, in (D) and (E).

(F and G) Comparison of DED1/DED2 interaction with the Pelle DD/Tube DD interaction. Pelle and Tube in the Pelle/Tube complex are each superimposed with DED1, respectively, in (F) and (G).

However, because DED1 is highly divergent from a typical DED fold, the interaction may not be representative of other DED/DED interactions. The interaction also differs from the two known modes of interaction within the DD superfamily, the interaction seen in the Pelle DD/Tube DD complex (Xiao et al., 1999) and that in the Apaf-1 CARD/pro-caspase-9 CARD complex (Qin et al., 1999) (Figures 3D, 3E, 3F, and 3G). The interaction between Pelle and Tube is completely different, involving

the H4 region of Pelle and the H6 region of Tube as well as an interaction at the C-terminal tail of Tube. The Apaf-1 CARD/pro-caspase-9 CARD interaction is somewhat similar; instead of the H2 and H5 helices as in DED1, the H2 and H3 helices of Apaf-1 interact with the H1 and H4 helices of pro-caspase-9. Interestingly, these three cases of homotypic interactions within the DD superfamily are all asymmetric, in contrast to what might have been expected for homotypic interactions.

MC159 Mutants that Fail to Protect Cells from Apoptosis Do Not Form a Ternary Complex with Fas and FADD

Previous mutational studies on MC159 have suggested that FADD recruitment does not seem sufficient for its anti-apoptotic function because almost all MC159 mutants that were deficient in protecting cells from Fas and TNFR1-induced apoptosis appear to have retained their abilities to interact with FADD (Garvey et al., 2002a). Having established that FADD does not interact strongly with MC159 in the absence of Fas, we considered the possibility that the binary FADD/MC159 interaction may not serve as a good indicator for MC159 recruitment to the DISC. Instead, we used our in vitro assay of ternary complex formation with Fas and FADD to characterize these previously generated MC159 mutants (Table 2). Strikingly, all tested mutants that failed to protect cells from apoptosis, including M2, M3, M5, M6, M8, M16, M17, M21, and M24, were also unable to form ternary complexes with Fas and FADD (Figure S1, lanes 2, 4, 6, 11, 15, 13, 17, 19, and 24). In contrast, MC159 mutants that retained full or partial ability to protect cells, such as M7, M9, M10, M18, and M27, were able to form the ternary complex (Figure S1, lanes 28, 30, 32, 37, and 39). Therefore, the ability of MC159 to protect cells from apoptosis is closely correlated with its recruitment to Fas and FADD. Hence, in contrast to previous suggestion, it appears that DISC recruitment of MC159 is both necessary and sufficient for its apoptotic protection function.

The DED2 Hydrophobic Patch of Caspase-8 Is Required for FADD Interaction

The MC159 structure provides a template for examining the structure and function relationships of tandem DED-containing proteins. Because earlier mutagenesis experiments on FADD showed that its hydrophobic patch, comprised of the conserved F25 and L26 residues, is important for caspase-8 recruitment (Eberstadt et al., 1998), we speculated that the same hydrophobic patch on caspase-8 may be involved in FADD association. Because the corresponding hydrophobic patch on DED1 is buried at the DED1/DED2 interface, only one conserved hydrophobic patch is present on tandem DED structures (Figures 2C and 3A). To elucidate whether this conserved hydrophobic patch of DED2 is involved in interaction with FADD, we performed an immunoprecipitation between caspase-8 and FADD (Figure 4A). An active site mutant of caspase-8 (C360S) was used to avoid caspase-8 autoprocessing. As predicted, the single site hydrophobic patch mutant of caspase-8, F122G, exhibited weakened interaction with FADD. The double mutant, F122G and L123G, completely abolished its interaction with FADD, demonstrating that these surface-exposed hydrophobic residues are absolutely required for the interaction of caspase-8 with FADD.

The DED2 Hydrophobic Patch of MC159 Is Not Required for Ternary Complex Formation, and MC159 Does Not Compete with Caspase-8 for DISC Recruitment

To determine whether the same hydrophobic patch on DED2 of MC159 is also important for MC159's recruitment, we examined the ability of the hydrophobic-patch

Table 2. Characterization of Previously Generated, Denoted as M Followed by a Number, and Additional, Denoted as MC Followed by a Number, MC159 Mutants for Ternary Complex Formation with Fas and FADD

Name	Mutation Sites ^a	Ternary Complex Formation	Apoptosis Protection ^a
M2	H23A, E24A, D25A	–	–
M3	H33A, D34A	–	–
M5	E62A	–	–
M6	R69A, D71A	–	–
M7	K81A, E82A	+	+
M8	R95A, R97A	–	–
M9	E105A, E106A	±	±
M10	R135A, E138A	+	+
M16	E18A, E19A, D21A	–	–
M17	F30A	–	–
M18	E111A, R113A	±	+
M21	L72A, L73A	–	–
M24	L31A	–	–
M27	M160A, L161A	+	±
M29	L157A	–	±
MC1	S9A, L10A, P11A, F12A	+	
MC2	E24D	+	
MC3	E24Q	–	
MC4	P37A	+	
MC5	T40A, T41A, T43A, Q44A	–	
MC6	C47A, S48A	+	
MC7	S50A, Q51A, Q52A	+	
MC8	Q51A, Q52A	+	
MC9	T56A, L57A	–	
MC10	Q68A	+	
MC11	R69K	–	
MC12	D71N	–	
MC13	K74A, S75A	+	
MC14	L79A, S80A	–	
MC15	Q86A, L87A, L88A	+	
MC16	T94A, R95A	–	
MC17	D108A, S109A, S110A	+	
MC18	E111Q	±	
MC19	L117G	+	
MC20	F118G	+	
MC21	L117G, F118G	+	
MC22	C120A, N121A, L122A, N123A, P124A, S125A	–	
MC23	S127A, T128A	+	
MC24	S131A, E132A, S133A	+	
MC25	E144A, N145A	–	
MC26	V146, L148	+	
MC27	S150G, P151G	+	
MC28	S155, V156	+	
MC29	R166K	+	
MC30	D168N	+	
MC31	Q171A, Q172A	+	
MC32	V174A, E175A	+	

^aApoptosis protection data for previously generated mutants were as reported in (Garvey et al., 2002a). The mutation sites for the previously generated mutants were determined by resequencing of the mutant plasmids and are different in M8 (previously reported as R95A, Y96A, and R97A), M9 (previously reported as E105A, E106A, and D108A), and M18 (previously reported as E111A, L112A, and R113A).

mutants of MC159 to form ternary complexes with Fas and FADD. In contrast to the requirement for the DED2 hydrophobic patch in caspase-8 recruitment, both single (L117G, F118G) and double (L117G and F118G) hydrophobic-patch mutants of MC159 had essentially no effect on its ability to form a ternary complex with

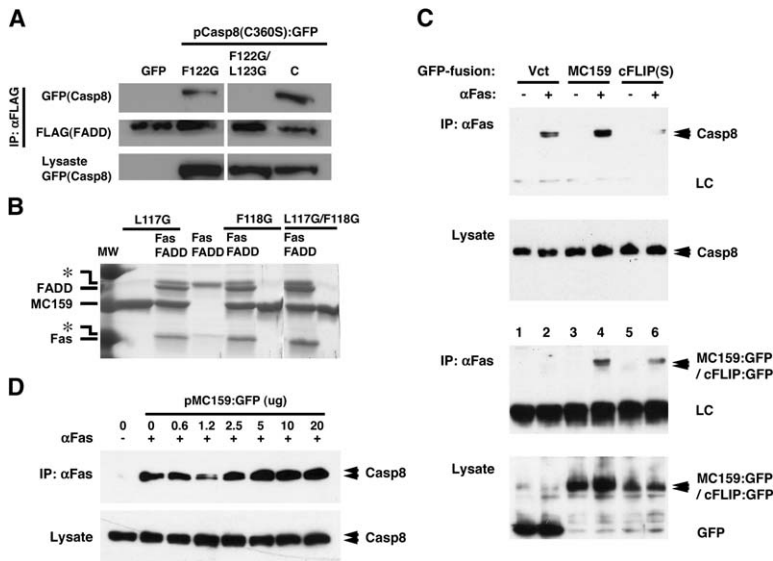


Figure 4. The Hydrophobic Patch of Caspase-8, but Not MC159, Is Involved in FADD Interaction, and MC159 Does Not Compete with Caspase-8 Recruitment

(A) Immunoprecipitation of wild-type and hydrophobic patch mutants of caspase-8 (C360S) and FADD is shown. (B) Ternary complex formation of hydrophobic patch mutants of MC159 with Fas and FADD. Contaminating bands are indicated by an asterisk. Please note that the last two lanes were cut and pasted from another gel. (C) MC159 does not compete with caspase-8 recruitment. Human lymphoma H9 cells were transfected with GFP-fusion constructs for expressing GFP (Vct), MC159:GFP, and cFLIP(S):GFP as indicated. The DISC was induced by anti-Fas stimulation as indicated, and its components were detected from the immunoprecipitates and cell lysates by probing against caspase-8 (upper panels) and GFP (lower panels). Please note that the last lane of the lysates was cut and pasted due to misloading in sample lanes. Data are representative of two independent experiments. (D) Caspase-8 recruitment in the presence of increasing amounts of MC159 transfection is shown.

Fas and FADD (Figure 4B). This suggests that the hydrophobic patch is not required for MC159 recruitment.

To elucidate whether MC159 competes with caspase-8 for recruitment to FADD, we performed a DISC assay in H9 cells with either GFP-MC159 or GFP-cFLIP(S) transfection. Upon stimulation by anti-Fas antibody, the cell lysates were immunoprecipitated, resolved by sodium dodecyl-sulfate-polyacrylamide gel electrophoresis (SDS-PAGE) and probed with either anti-caspase-8 or anti-GFP antibodies. Whereas cFLIP(S) transfection strongly inhibited caspase-8 recruitment, MC159 transfection did not attenuate caspase-8 recruitment to the DISC (Figure 4C). In fact, a detailed titration on the transfection of GFP-MC159 fusion plasmid indicated that MC159 might have subtly enhanced caspase-8 recruitment (Figure 4D). These and the hydrophobic patch mutation data suggest that caspase-8 and MC159 apparently utilize different structural features for FADD interaction.

An Extensive Surface of MC159 and the Charge Triad Region of FADD Are Both Required for Ternary Complex Formation

Among the previously generated MC159 mutants, most are on buried residues and therefore may cause structural perturbations. Only M2 (H23A, E24A, and D25A), M3 (H33A, D34A), M6 (R69A, D71A), and M16 (E18A, E19A, and D21A) contain surface-exposed residues and are defective in protection against apoptosis (Table 2). These residues may directly participate in FADD interaction. To thoroughly map the molecular determinants of MC159 recruitment, we generated 32 additional MC159 mutants on surface-exposed residues, most of which contain charged or large (either hydrophobic or hydrophilic) side chains. We characterized them with the *in vitro* assay on ternary complex formation. Nine out of the 32 mutants were defective in ternary complex formation (Table 2).

Mapping of MC159 mutations that were defective in ternary complex formation (Figure 3A) showed the involvement of an extensive region of the structure in its recruitment (Figure 5A). This suggests that each MC159 may contact at least two adjacent FADD molecules. On one side of the structure, a region near the charge triad in DED1, which comprises mutants M2 (H23A, E24A, and D25A), M6 (R69A and D71A), M16 (E18A, E19A, and D21A), and MC5 (T40A, T41A, T43A, and Q44A), is important (Figure 5B). For residues within the charge triad in this region, even the very conserved substitutions E24Q, R69K, and D71N abolished ternary complex formation. On the same side of the structure, the charge triad in DED2 does not seem to be as important, as E111Q, R166K, and D168N mutations at worst weakened ternary complex formation. Therefore, on this side of the MC159 structure, it appears only DED1 is important for its recruitment. Most of the remaining mutations map to the opposite face of MC159 (Figure 5C). They comprise mutants M3 (H33A and D34A), MC9 (T56A and L57A), MC14 (L79A and S80A), MC16 (T94A and R95A), MC22 (C120A, N121A, L122A, N123A, P124A, and S125A), and MC25 (E144A and N145A). Residues from both DED1 and DED2 participate in interactions at this side.

The importance of the charge triad of MC159 in FADD interaction suggests that the same charge triad region of FADD may be reciprocally important for interaction with MC159. To test this hypothesis, we performed site-directed mutagenesis on the charge triad region of FADD, R72E, and D74K and tested the ability of these FADD mutants to form a ternary complex with MC159. As predicted, mutants R72E and D74K completely abolished and weakened ternary complex formation, respectively (data not shown), suggesting that the charge triad region of FADD is involved in MC159 recruitment (Figure 5D).

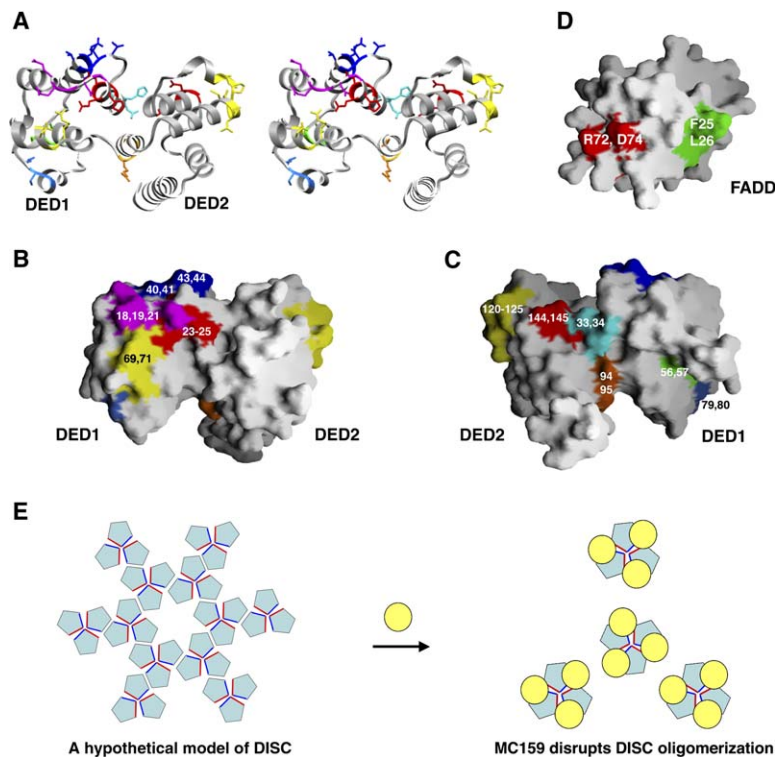


Figure 5. Interaction between MC159 and FADD and a Proposed Model for the Inhibition of Caspase Activation by MC159

(A) Mapping of surface mutations of MC159 that are defective in FADD interaction onto the stereo ribbon diagram of its structure. Residues E18, E19, and D21, magenta; H23, E24, and D25, red; H33 and D34, cyan; T40, T41, T43, and Q44: dark blue; T56 and L57, green; R69 and D71, yellow; L79 and S80, blue; T94 and R95, gold; C120, N121, L122, N123, P124, and S125, yellow; E145 and N145, red.

(B and C) Mapping of the same mutations onto the molecular surface of MC159 is shown. Residue numbers are shown. (B) is shown in the same orientation as in (A), and (C) is related to (A) by a 180° rotation about the vertical axis.

(D) Mapping of FADD mutations R72E and D74K, within the charge triad, onto its surface. The location of the conserved hydrophobic patch (F25 and L26) is also shown.

(E) A proposed model for the inhibition of caspase activation at the DISC by MC159 via disruption of FADD self-association. The pentagons represent monomeric Fas/FADD/caspase-8 complexes, and filled yellow circles represent MC159 molecules. The Fas/FADD/caspase-8 complexes likely interact with each other via both trimeric associations, as dictated by trimeric FasL, and dimeric associations

from FADD self-association. Schematically, the blue and red faces of the pentagons mediate trimeric associations, and the face adjacent to the blue mediates dimeric associations. These two types of associations could mediate the infinite oligomerization of DISC during signaling. MC159 likely interacts with at least two neighboring FADD molecules and disrupts DISC oligomerization by competing with the same face used for the dimeric FADD self-association.

Discussion

Cooperative Ternary Complex Assembly in Caspase-8 and MC159 Recruitment

By using recombinant proteins, we showed that Fas DD, FADD, and MC159 are cooperatively assembled. Similarly, the ternary complex of Fas DD, FADD, and caspase-8 are also cooperatively assembled (data not shown). These molecular assembly processes likely recapitulate the early event in Fas signaling *in vivo*, the formation of the signaling protein oligomeric transduction structures (SPOTS) (Siegel *et al.*, 2004). Like the ternary complex formation, assembly of SPOTS is absolutely dependent on Fas DD and FADD and is enhanced by caspase-8, regardless of its catalytic activity (Siegel *et al.*, 2004). Because it is detrimental to activate caspases in the absence of distinct signaling events, this cooperative assembly appears to act as a safety measure in preventing accidental DISC formation. Other oligomeric death-inducing complexes such as complex II formed by TRADD, FADD, and caspase-8 (Micheau and Tschopp, 2003) and PIDDosome formed by PIDD, RAIDD, and caspase-2 (Tinel and Tschopp, 2004) likely obey the same assembly mechanism.

MC159 as a Template for Tandem DED Structures

Unlike beads on a string, DED1 and DED2 are rigidly associated to form a single compact structure in which each domain performs its unique structural role in the context of the tandem DEDs and is not interchangeable in position with the other. This integral structure of tandem DEDs explains the previous observation that both

DEDs of MC159 are required for its antiapoptotic function (Garvey *et al.*, 2002a). On an isolated domain level, DED1 and DED2 differ significantly. Whereas DED2 appears to be a bona fide DED and closely resembles the DED structures in FADD (Eberstadt *et al.*, 1998) and PEA-15 (Hill *et al.*, 2002), DED1 appears to be equally distant to these known DED structures as to other structures in the DD superfamily such as DDs, PYDs, and CARDS. The association between DED1 and DED2 in tandem DEDs reveals a mode of interaction between DEDs that differs significantly from observed CARD/CARD and DD/DD interactions.

Structural analyses reveal two distinctive surface features in DED structures. The first feature is the conserved hydrophobic patches. In DED1, this conserved hydrophobic patch is used to support the DED1/DED2 interface and is buried at this interface. In contrast, the conserved DED2 hydrophobic patch is surface exposed and available for interactions. The second distinctive surface feature is the conserved hydrogen-bonded charge triad, which we refer to here as the E/D-RxDL motif. It is a signature of DEDs and is not present in DDs, CARDS, or PYDs. This region of the DED surface also appears to be a hot spot for protein-protein interactions.

Molecular Mechanism for the Recruitment of Caspase-8, and Possibly Caspase-10, cFLIPs and Herpesvirus vFLIPs: the Conserved Hydrophobic Patch

The first structure of a tandem DED-containing protein provides a template for understanding the molecular basis of procaspase recruitment and FLIP inhibition during

DR signaling. The conserved hydrophobic patch on DEDs was first identified from the NMR structure of FADD, which comprises two central large hydrophobic residues, F25 and L26 (Eberstadt et al., 1998). It was shown to be important for the interaction of FADD with caspase-8. Here, we show that the conserved DED2 hydrophobic patch of caspase-8 is important for its recruitment to FADD.

We speculate that the use of the hydrophobic patch for DISC recruitment is likely to be true for caspase-10, cFLIP, and herpesvirus vFLIPs as well. In these tandem DED-containing proteins, the Phe residue in the hydrophobic patch is strictly conserved as Phe or Tyr, and the Leu residue is strictly conserved as Leu or Ile (Figure 3A) (Tibbetts et al., 2003). Therefore, cFLIP would compete directly with caspase-8 for DISC recruitment, as shown here (Figure 4C). In addition, herpesvirus vFLIPs would also likely inhibit caspase activation by direct competition with caspase-8 for DISC recruitment.

However, this scenario is not true for MC159. As we've shown here, mutations of the DED2 hydrophobic patch residues did not affect MC159 recruitment. The lack of involvement of the hydrophobic patch in MC159 recruitment may be rationalized by its less-conserved substitutions at this site; the conserved Phe is replaced by a Leu and the conserved Leu is replaced by a Phe. In FADD, it appears that the Phe position has to be an aromatic residue as changes to Tyr and Trp retained its ability to interact with caspase-8, whereas a change to Val abolished the interaction (Eberstadt et al., 1998). It is likely then that the Phe to Leu substitution in MC159 also abolishes its interaction with the hydrophobic patch of FADD. The same Phe to Leu change is also observed in MC160, another vFLIP-like protein from MCV (Shisler and Moss, 2001). The only other DED-containing protein that does not have the conserved hydrophobic patch is PEA-15, a protein not involved in death receptor signaling and regulation.

Molecular Mechanism for MC159 Recruitment and Inhibition of Caspase Activation: the Charge Triad and the Disruption of FADD Self-Association

In contrast to the involvement of the hydrophobic patch, we have shown here that MC159 uses an extensive surface encompassing the charge triad for interaction with FADD. This is consistent with the previous observation that the RxDL motifs of MC159 play important roles in MC159 function (Garvey et al., 2002a). The extensive nature of the interaction surface suggests that each MC159 contacts at least two adjacent FADD molecules. Reciprocally, we showed that the charge triad of FADD is important for interaction with MC159. However, because MC159 does not compete with caspase-8 for recruitment, how does it inhibit caspase activation and apoptosis?

To answer this question, we have to analyze the basic requirement for DISC assembly. Because FasL is intrinsically trimeric, the assembled DISC should at least be trimeric. In addition, because FADD self-associates, higher order of aggregation is generated. If we assume that FADD self-associates via a dimeric interaction, this dimerization of trimers would provide a mode of infinite aggregation (Figure 5E) into variably sized SPOTS that are observable under a light microscope. This exist-

tence of the dimeric symmetry would be consistent with the requirement for dimerization in caspase-8 activation (Boatright et al., 2003; Donepudi et al., 2003). In addition, the formation of higher-order oligomers is essential for caspase activation as trimeric soluble FasL is rather inefficient in inducing caspase activation whereas hexameric FasL is much more efficient (Holler et al., 2003).

Interestingly, we have recently shown that FADD also self-associates via the RxDL motif in the charge triad region (Muppidi et al., 2005). Therefore, MC159 would compete with and disrupt FADD self-association. In the absence of FADD self-association, higher-order oligomerization of DISC would be abolished and, therefore, caspase activation would be inhibited (Figure 5E). This model of MC159 function elegantly explains the molecular basis for its antiapoptotic activity. It is supported by the observation that MC159 reduces the size of SPOTS during Fas signaling (Siegel et al., 2004). Similarly, it blocks the formation of FADD "death effector filaments," which are self-oligomerized FADD molecules upon overexpression, and inhibits caspase activation and apoptosis (Garvey et al., 2002b; Siegel et al., 1998). Therefore, unlike cFLIPs and herpesvirus vFLIPs, MC159 uses a noncompetitive mechanism for inhibiting caspase activation at the DISC level.

Experimental Procedures

Protein Expression and Purification

MC159 from *Molluscum contagiosum* virus (residues 1–241 and residues 1–187) was expressed as His-tagged proteins in *E. coli* by using 20°C induction and was purified by Ni-affinity and gel filtration chromatography. Human Fas DD, human FADD, human FADD DD, and human FADD DED proteins, either His-tagged or with no tags, were expressed similarly by using low temperature inductions. FADD and FADD DED constructs both contain the F25Y mutation that retains FADD function but improves its solution behavior (Eberstadt et al., 1998).

Crystallization and Structure Determination of MC159

Selenomethionine-substituted full-length MC159 was crystallized with the hanging drop vapor diffusion method under 50–150 mM sodium and potassium phosphate at pH 5.0. The crystals were highly variable; upon screening many crystals, a single-wavelength anomalous diffraction data set was collected at 3.8 Å resolution with the SGX ID beam line at the Advanced Photon Source (Table 1). Diffraction data were processed and scaled by using HKL2000 software (Otwinowski and Minor, 1997). The crystal belongs to space group P22₂, with cell dimensions of a = 84.0 Å, b = 108.2 Å, and c = 142.7 Å. Selenium sites were determined with direct method calculations in SnB (Weeks and Miller, 1999) and fed into SOLVE (Terwilliger, 2004) for phase determination. In combination with 4-fold non-crystallographic symmetry averaging in RESOLVE (Terwilliger, 2004), an interpretable map was obtained. Facilitated by the known selenium sites as markers for methionine residues, all four molecules in the crystallographic asymmetric unit were traced and built (residues 2–187) by using O (Jones et al., 1991).

The structure revealed that a large segment of the C-terminal tail (residues 188–241) is disordered in the crystal. This C-terminal tail is not important for the function of MC159 (Garvey et al., 2002a). Another construct (residues 1–187), made based on the ordered part of the molecule, gave soluble proteins and was crystallized with the hanging-drop vapor-diffusion method under 1.0–1.2 M sodium acetate in 0.1 M imidazole at pH 6.5. The crystals belong to space group P2₁2₁2₁ and diffracted beyond 1.2 Å resolution at the X4A beamline of the National Synchrotron Light Source (NSLS). The structure was determined by molecular replacement calculations in COMO (JogI et al., 2001) by using the partially refined model from the initial crystal form. All crystallographic refinement calculations were performed in CNS (Brunger et al., 1998), and the structures were analyzed and

displayed with Setor (Evans, 1993), Molscript/Raster3D (Kraulis, 1991; Merritt and Murphy, 1994), and Grasp software (Nicholls et al., 1991).

Mutagenesis and His-Tag Pull-Down

Mutagenesis of MC159 was performed with the QuikChange Site-Directed Mutagenesis Kit (Stratagene). Wild-type and mutant His-tagged MC159 proteins were first purified with Ni-affinity to assess their expression levels. Then, cell lysates containing estimated equivalent quantities of MC159 proteins were mixed with those of nontagged Fas DD and FADD. The mixtures were incubated at room temperature for 2 hours, and His-tag pull-down experiments were performed to determine whether they form ternary complexes with Fas and FADD.

Immunoprecipitation and Western Blot

Human embryonic kidney tumor line 293T cells were seeded at 10^6 well in complete Dulbecco's modified Eagle's medium (DMEM) in six well plates and cultured overnight. The cells were transfected with 3 μ g of plasmid DNA by using Fugene 6 (Roche) reagent according to the manufacturer's instructions. The cells were cultured for 24 to ~48 hours, harvested, and lysed on ice by 0.5 ml of the TNTG lysis buffer (30 mM Tris-HCl [pH 8.0], 150 mM NaCl, 1% Triton X-100, and 10% glycerol) with 1 \times protease inhibitor cocktail (Roche) for 30 minutes. The lysates were centrifuged at 10,000 \times g at 8°C for 10 minutes. The protein-normalized lysates were subjected to immunoprecipitation by adding 10 μ g/ml appropriate antibody, 30 μ l of protein G-agarose (Roche), and rotating for more than 2 hr in the cold room. The precipitates were washed five times with cold TNTG lysis buffer and then subjected to 4% to ~20% Tris/Glycine-SDS PAGE under reduced and denaturing conditions. The resolved protein bands were transferred onto nitrocellulose membranes and probed with 1 mg/ml of appropriate primary antibodies in PBS-T (phosphate-buffered saline with 0.1% Tween-20) at room temperature for 2 hr and then with appropriate HRP-conjugated secondary antibodies for 1 hr. The blots were then developed by the SuperSignaling system (Pierce) according to the manufacturer's instructions.

For DISC assay, 8×10^6 human lymphoma H9 cells were transfected with up to 20 μ g of plasmid by electroporation with the BTX Electro Cell Manipulator 600. The transfected cells were cultured in 10 ml of complete RPMI medium for 36 hr, and viable cells were purified by gradient centrifugation. Each of 5×10^6 transfected cells was subjected to mock or anti-Fas (Apo-1.3, 1 μ g/ml) stimulation for 10 min at 37°C. The stimulated cells were washed twice with cold PBS followed by the immunoprecipitation and Western blotting protocols described above.

Supplemental Data

Supplemental Data including one figure and two tables are available online with this article at <http://www.molecule.org/cgi/content/full/20/6/939/DC1/>.

Acknowledgments

We thank Dr. Stephen R. Wasserman for the use of SGX-CAT at Sector 31 of the Advanced Photon Source, which was constructed and operated by Structural GenomiX, Inc.; Randy Abramowitz and John Schwanof for use of the X4A beamline at NSLS; Dr. Jeffrey Cohen for providing MC159 mutants; and Samantha Jayawickrama for some of the mutagenesis work. J.K.Y. is a postdoctoral fellow of the Serono Foundation. L.X.Z., F.Y.W., and M.J.L. are supported by the Intramural Research Program of the National Institute of Allergy and Infectious Diseases, NIH. This work was supported by NIH grant R01 AI-50872 to H.W.

Received: September 11, 2005

Revised: October 18, 2005

Accepted: October 19, 2005

Published: December 21, 2005

References

Bertin, J., Armstrong, R.C., Otilie, S., Martin, D.A., Wang, Y., Banks, S., Wang, G.H., Senkevich, T.G., Alnemri, E.S., Moss, B., et al. (1997).

Death effector domain-containing herpesvirus and poxvirus proteins inhibit both Fas- and TNFR1-induced apoptosis. *Proc. Natl. Acad. Sci. USA* 94, 1172–1176.

Boatright, K.M., Renatus, M., Scott, F.L., Sperandio, S., Shin, H., Pedersen, I.M., Ricci, J.E., Edris, W.A., Sutherlin, D.P., Green, D.R., and Salvesen, G.S. (2003). A unified model for apical caspase activation. *Mol. Cell* 11, 529–541.

Boldin, M.P., Goncharov, T.M., Goltsev, Y.V., and Wallach, D. (1996). Involvement of MACH, a novel MORT1/FADD-interacting protease, in Fas/APO-1- and TNF receptor-induced cell death. *Cell* 85, 803–815.

Brunger, A.T., Adams, P.D., Clore, G.M., DeLano, W.L., Gros, P., Grosse-Kunstleve, R.W., Jiang, J.S., Kuszewski, J., Nilges, M., Pannu, N.S., et al. (1998). Crystallography & NMR system: a new software suite for macromolecular structure determination. *Acta Crystallogr. D* 54, 905–921.

Chinnaiyan, A.M., O'Rourke, K., Tewari, M., and Dixit, V.M. (1995). FADD, a novel death domain-containing protein, interacts with the death domain of Fas and initiates apoptosis. *Cell* 81, 505–512.

Chou, J.J., Matsuo, H., Duan, H., and Wagner, G. (1998). Solution structure of the RAIDD CARD and model for CARD/CARD interaction in caspase-2 and caspase-9 recruitment. *Cell* 94, 171–180.

Donepudi, M., Mac Sweeney, A., Briand, C., and Grutter, M.G. (2003). Insights into the regulatory mechanism for caspase-8 activation. *Mol. Cell* 11, 543–549.

Eberstadt, M., Huang, B., Chen, Z., Meadows, R.P., Ng, S.-C., Zheng, L., Lenardo, M.J., and Fesik, S.W. (1998). NMR structure and mutagenesis of the FADD (Mort1) death-effector domain. *Nature* 392, 941–945.

Evans, S.V. (1993). SETOR: hardware-lighted three-dimensional solid model representations of macromolecules. *J. Mol. Graph.* 11, 134–138.

French, L.E., and Tschopp, J. (2003). Protein-based therapeutic approaches targeting death receptors. *Cell Death Differ.* 10, 117–123.

Garvey, T.L., Bertin, J., Siegel, R., Lenardo, M., and Cohen, J. (2002a). The death effector domains (DEDs) of the molluscum contagiosum virus MC159 v-FLIP protein are not functionally interchangeable with each other or with the DEDs of caspase-8. *Virology* 300, 217–225.

Garvey, T.L., Bertin, J., Siegel, R.M., Wang, G.H., Lenardo, M.J., and Cohen, J. (2002b). Binding of FADD and caspase-8 to molluscum contagiosum virus MC159 v-FLIP is not sufficient for its antiapoptotic function. *J. Virol.* 76, 697–706.

Goltsev, Y.V., Kovalenko, A.V., Arnold, E., Varfolomeev, E.E., Brodianskii, V.M., and Wallach, D. (1997). CASH, a novel caspase homologue with death effector domains. *J. Biol. Chem.* 272, 19641–19644.

Han, D.K., Chaudhary, P.M., Wright, M.E., Friedman, C., Trask, B.J., Riedel, R.T., Baskin, D.G., Schwartz, S.M., and Hood, L. (1997). MRIT, a novel death-effector domain-containing protein, interacts with caspases and BclXL and initiates cell death. *Proc. Natl. Acad. Sci. USA* 94, 11333–11338.

Hill, J.M., Vaidyanathan, H., Ramos, J.W., Ginsberg, M.H., and Werner, M.H. (2002). Recognition of ERK MAP kinase by PEA-15 reveals a common docking site within the death domain and death effector domain. *EMBO J.* 21, 6494–6504.

Hiller, S., Kohl, A., Fiorito, F., Herrmann, T., Wider, G., Tschopp, J., Grutter, M.G., and Wuthrich, K. (2003). NMR structure of the apoptosis- and inflammation-related NALP1 pyrin domain. *Structure (Camb)* 11, 1199–1205.

Holler, N., Tardivel, A., Kovacovics-Bankowski, M., Hertig, S., Gaide, O., Martinon, F., Tinel, A., Deperthes, D., Calderara, S., Schulthess, T., et al. (2003). Two adjacent trimeric Fas ligands are required for Fas signaling and formation of a death-inducing signaling complex. *Mol. Cell. Biol.* 23, 1428–1440.

Holm, L., and Sander, C. (1995). Dali: a network tool for protein structure comparison. *Trends Biochem. Sci.* 20, 478–480.

Hu, S., Vincenz, C., Buller, M., and Dixit, V.M. (1997a). A novel family of viral death effector domain-containing molecules that inhibit both CD-95- and tumor necrosis factor receptor-1-induced apoptosis. *J. Biol. Chem.* 272, 9621–9624.

- Hu, S., Vincenz, C., Ni, J., Gentz, R., and Dixit, V.M. (1997b). I-FLICE, a novel inhibitor of tumor necrosis factor receptor-1- and CD-95-induced apoptosis. *J. Biol. Chem.* **272**, 17255–17257.
- Huang, B., Eberstadt, M., Olejniczak, E.T., Meadows, R.P., and Fesik, S.W. (1996). NMR structure and mutagenesis of the Fas (APO-1/CD95) death domain. *Nature* **384**, 638–641.
- Inohara, N., Koseki, T., Hu, Y., Chen, S., and Nunez, G. (1997). CLARP, a death effector domain-containing protein interacts with caspase-8 and regulates apoptosis. *Proc. Natl. Acad. Sci. USA* **94**, 10717–10722.
- Irmiler, M., Thome, M., Hahne, M., Schneider, P., Hofmann, K., Steiner, V., Bodmer, J.L., Schroter, M., Burns, K., Mattmann, C., et al. (1997). Inhibition of death receptor signals by cellular FLIP. *Nature* **388**, 190–195.
- Itoh, N., and Nagata, S. (1993). A novel protein domain required for apoptosis. Mutational analysis of human Fas antigen. *J. Biol. Chem.* **268**, 10932–10937.
- Jogl, G., Tao, X., Xu, Y., and Tong, L. (2001). COMO: a program for combined molecular replacement. *Acta Crystallogr. D Biol. Crystallogr.* **57**, 1127–1134.
- Jones, T.A., Zou, J.-Y., Cowan, S.W., and Kjeldgaard, M. (1991). Improved methods for building models in electron density maps and the location of errors in those models. *Acta Crystallogr. A* **47**, 110–119.
- Kischkel, F.C., Hellbardt, S., Behrmann, I., Germer, M., Pawlita, M., Kramer, P.H., and Peter, M.E. (1995). Cytotoxicity-dependent APO-1 (Fas/CD95)-associated proteins form a death-inducing signaling complex (DISC) with the receptor. *EMBO J.* **14**, 5579–5588.
- Kohl, A., and Grutter, M.G. (2004). Fire and death: the pyrin domain joins the death-domain superfamily. *C. R. Biol.* **327**, 1077–1086.
- Kraulis, P.J. (1991). MOLSCRIPT: a program to produce both detailed and schematic plots of protein structures. *J. Appl. Crystallogr.* **24**, 946–950.
- Locksley, R.M., Killeen, N., and Lenardo, M.J. (2001). The TNF and TNF receptor superfamilies: integrating mammalian biology. *Cell* **104**, 487–501.
- Medema, J.P., Scaffidi, C., Kischkel, F.C., Shevchenko, A., Mann, M., Kramer, P.H., and Peter, M.E. (1997). FLICE is activated by association with the CD95 death-inducing signaling complex (DISC). *EMBO J.* **16**, 2794–2804.
- Merritt, E.A., and Murphy, M.E. (1994). Raster3D Version 2.0. A program for photorealistic molecular graphics. *Acta Crystallogr. D Biol. Crystallogr.* **50**, 869–873.
- Micheau, O., and Tschopp, J. (2003). Induction of TNF receptor I-mediated apoptosis via two sequential signaling complexes. *Cell* **114**, 181–190.
- Muppidi, J.R., Lobito, A.A., Ramaswamy, M., Yang, J.K., Wang, L., Wu, H., and Siegel, R.M. (2005). Homotypic FADD interactions through a conserved RXDLL motif are required for death receptor-induced apoptosis. *Cell Death Differ.*, in press.
- Muzio, M., Chinnaiyan, A.M., Kischkel, F.C., O'Rourke, K., Shevchenko, A., Ni, J., Scaffidi, C., Bretz, J.D., Zhang, M., Gentz, R., et al. (1996). FLICE, a novel FADD-homologous ICE/CED-3-like protease, is recruited to the CD95 (Fas/APO-1) death-inducing signaling complex. *Cell* **85**, 817–827.
- Nicholls, A., Sharp, K.A., and Honig, B. (1991). Protein folding and association: insights from the interfacial and thermodynamic properties of hydrocarbons. *Proteins* **11**, 281–296.
- Otwinowski, Z., and Minor, W. (1997). Processing of X-ray diffraction data collected in oscillation mode. *Methods Enzymol.* **276**, 307–326.
- Peter, M.E., and Kramer, P.H. (2003). The CD95(APO-1/Fas) DISC and beyond. *Cell Death Differ.* **10**, 26–35.
- Qin, H., Srinivasula, S.M., Wu, G., Fernandes-Alnemri, T., Alnemri, E.S., and Shi, Y. (1999). Structural basis of procaspase-9 recruitment by the apoptotic protease-activating factor 1. *Nature* **399**, 549–557.
- Rasper, D.M., Vaillancourt, J.P., Hadano, S., Houtzager, V.M., Seiden, I., Keen, S.L., Tawa, P., Xanthoudakis, S., Nasir, J., Martindale, D., et al. (1998). Cell death attenuation by 'Usurpin', a mammalian DED-caspase homologue that precludes caspase-8 recruitment and activation by the CD-95 (Fas, APO-1) receptor complex. *Cell Death Differ.* **5**, 271–288.
- Reed, J.C., Doctor, K.S., and Godzik, A. (2004). The domains of apoptosis: a genomics perspective. *Sci. STKE* **29**, re9.
- Salvesen, G.S. (2002). Caspases and apoptosis. *Essays Biochem.* **38**, 9–19.
- Salvesen, G.S., and Dixit, V.M. (1999). Caspase activation: the induced-proximity model. *Proc. Natl. Acad. Sci. USA* **96**, 10964–10967.
- Searles, R.P., Bergquam, E.P., Axthelm, M.K., and Wong, S.W. (1999). Sequence and genomic analysis of a Rhesus macaque rhadinovirus with similarity to Kaposi's sarcoma-associated herpesvirus/human herpesvirus 8. *J. Virol.* **73**, 3040–3053.
- Shi, Y. (2004). Caspase activation: revisiting the induced proximity model. *Cell* **117**, 855–858.
- Shisler, J.L., and Moss, B. (2001). Molluscum contagiosum virus inhibitors of apoptosis: The MC159 v-FLIP protein blocks Fas-induced activation of procaspases and degradation of the related MC160 protein. *Virology* **282**, 14–25.
- Shu, H.B., Halpin, D.R., and Goeddel, D.V. (1997). Casper is a FADD- and caspase-related inducer of apoptosis. *Immunity* **6**, 751–763.
- Siegel, R.M., Martin, D.A., Zheng, L., Ng, S.Y., Bertin, J., Cohen, J., and Lenardo, M.J. (1998). Death-effector filaments: novel cytoplasmic structures that recruit caspases and trigger apoptosis. *J. Cell Biol.* **141**, 1243–1253.
- Siegel, R.M., Muppidi, J.R., Sarker, M., Lobito, A., Jen, M., Martin, D., Straus, S.E., and Lenardo, M.J. (2004). SPOTS: signaling protein oligomeric transduction structures are early mediators of death receptor-induced apoptosis at the plasma membrane. *J. Cell Biol.* **167**, 735–744.
- Srinivasula, S.M., Ahmad, M., Otilie, S., Bullrich, F., Banks, S., Wang, Y., Fernandes-Alnemri, T., Croce, C.M., Litwack, G., Tomaselli, K.J., et al. (1997). FLAME-1, a novel FADD-like anti-apoptotic molecule that regulates Fas/TNFR1-induced apoptosis. *J. Biol. Chem.* **272**, 18542–18545.
- Tartaglia, L.A., Ayres, T.M., Wong, G.H., and Goeddel, D.V. (1993). A novel domain within the 55 kd TNF receptor signals cell death. *Cell* **74**, 845–853.
- Terwilliger, T. (2004). SOLVE and RESOLVE: automated structure solution, density modification and model building. *J. Synchrotron Radiat.* **11**, 49–52.
- Thome, M., and Tschopp, J. (2001). Regulation of lymphocyte proliferation and death by FLIP. *Nat. Rev. Immunol.* **1**, 50–58.
- Thome, M., Schneider, P., Hofmann, K., Fickenscher, H., Meinl, E., Neipel, F., Mattmann, C., Burns, K., Bodmer, J.L., Schroter, M., et al. (1997). Viral FLICE-inhibitory proteins (FLIPs) prevent apoptosis induced by death receptors. *Nature* **386**, 517–521.
- Tibbetts, M.D., Zheng, L., and Lenardo, M.J. (2003). The death effector domain protein family: regulators of cellular homeostasis. *Nat. Immunol.* **4**, 404–409.
- Tinel, A., and Tschopp, J. (2004). The PIDDosome, a protein complex implicated in activation of caspase-2 in response to genotoxic stress. *Science* **304**, 843–846.
- Wajant, H. (2002). The Fas signaling pathway: more than a paradigm. *Science* **296**, 1635–1636.
- Weeks, C.M., and Miller, R. (1999). Optimizing shake-and-bake for proteins. *Acta Crystallogr. D Biol. Crystallogr.* **55**, 492–500.
- Xiao, T., Towb, P., Wasserman, S.A., and Sprang, S.R. (1999). Three-dimensional structure of a complex between the death domains of Pelle and Tube. *Cell* **99**, 545–555.

Accession Numbers

The coordinates have been deposited in the RCSB Protein Data Bank with the PDB codes of [2BBZ](#) for the 3.8 Å resolution MC159 structure and [2BBR](#) for the 1.2 Å resolution MC159 structure.

Supplemental Data

Crystal Structure of MC159 Reveals Molecular Mechanism of DISC Assembly and FLIP Inhibition

Jin Kuk Yang, Liwei Wang, Lixin Zheng, Fengyi Wan, Misonara Ahmed, Michael J. Lenardo, and Hao Wu

Table S1. Structural Alignment and Homology Search

Structural Alignment				
	Name	Distance cutoff	# Residues Aligned	RMSD
DED1	DED2	3.0Å	51	1.3Å
	FADD DED	3.0Å	49	1.6Å
	PEA-15 DED	3.0Å	42	1.6Å
DED2	FADD DED	3.0Å	74	1.4Å
	PEA-15 DED	3.0Å	74	1.4Å
Structural Homology Search with DALI, Top 8 Matches				
	Name	Z score	# Residues Aligned	RMSD
DED1	FADD DED	6.2	71	2.5Å
	Pelle DD	5.8	78	3.0Å
	Nalp1 PYD	5.6	66	2.3Å
	p75 DD	5.3	71	2.8Å
	Asc PYD	5.2	70	2.5Å
	Iceberg CARD	5.1	71	2.5Å
	TNF-R1 DD	4.8	66	2.7Å
	P84 DD	4.7	71	2.7Å
DED2	FADD DED	11.6	82	1.8Å
	PEA-15 DED	10.8	92	2.4Å
	Asc PYD	9.0	83	2.4Å
	Caspase-9 CARD	7.4	78	2.3Å
	Iceberg CARD	7.1	76	3.1Å
	Pelle DD	6.9	77	2.9Å
	Nalp1 PYD	6.7	75	2.4Å
	p75 DD	6.7	73	2.6Å

Table S2. Charge Triad Defined by the E/D-RxDL Motif in DED1 and DED2 (in parenthesis)

Residue	Atom	Residue	Atom	Distance (Å)
R69 (R166)	N ϵ	D71 (D168)	O δ 1	2.9 (2.9)
R69 (R166)	N η 2	D71 (D168)	O δ 2	2.9 (2.9)
R69 (R166)	N η 1	E24 (E111)	O ϵ 1	3.3 (3.3)
R69 (R166)	N η 1	E24 (E111)	O ϵ 2	2.9 (2.8)

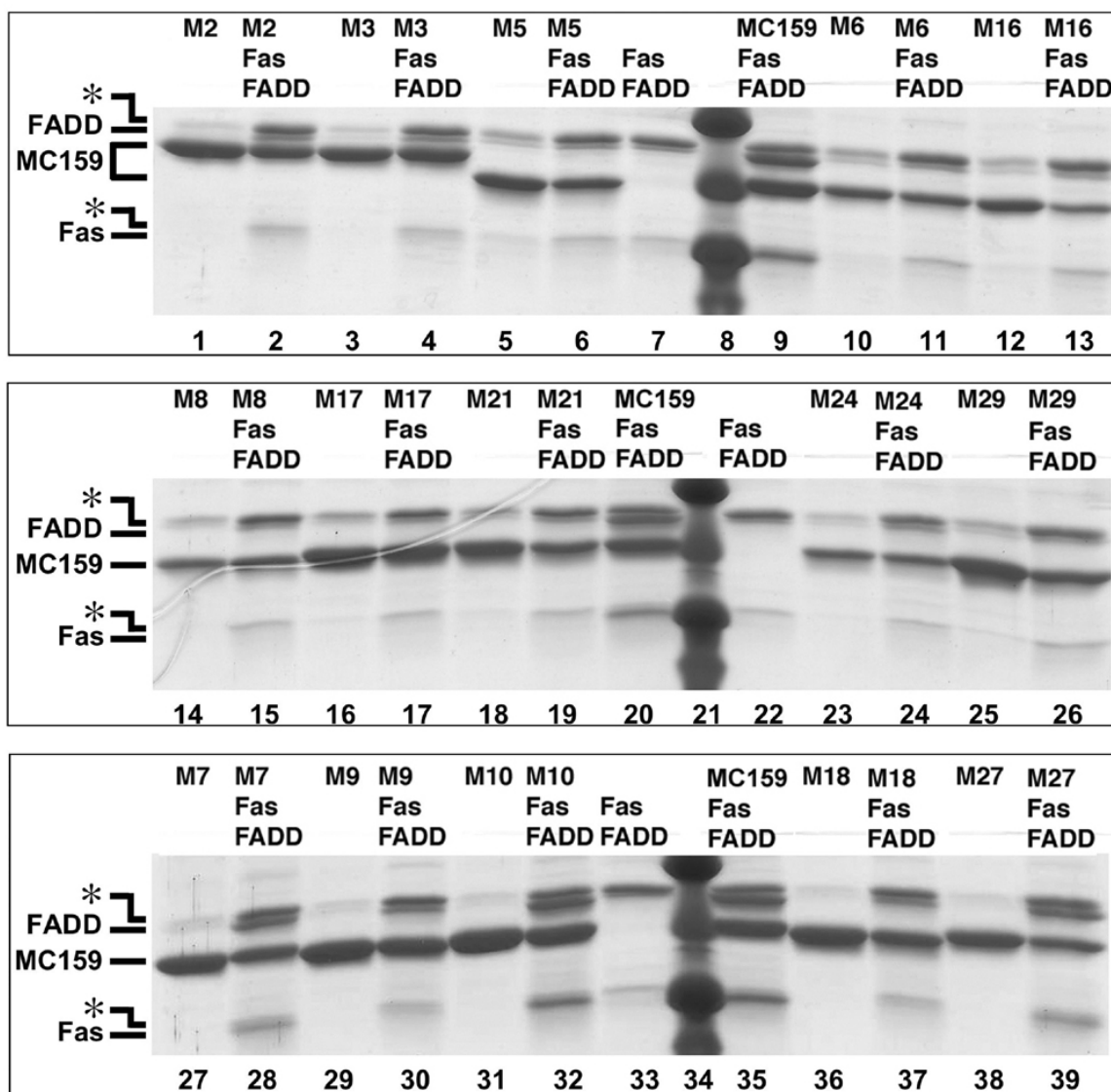


Figure S1. Characterization of MC159 Mutants Using His-tag Pull-Down

The definitions of the mutants are shown in Table 2. MC159 mutants M2 and M3 are of full-length MC159 (residues 1-241) while the remaining mutants are of truncated MC159 (residues 1-187). Contaminants are labeled by an asterisk.